IMTC 2008 – IEEE Instrumentation and Measurement
Technology Conference
Victoria, Canada, May 12–15, 2008

Vision-Based Control of an Inverted Pendulum using Cascaded Particle Filters

Manuel Stuflesser and Markus Brandner

Institute of Electrical Measurement and Measurement Signal Processing,
Graz University of Technology,
Kopernikusgasse 24/IV, A8010 Graz, Austria
E–mail: brandner@ieee.org

Abstract – *The inverted pendulum represents an example of a non-linear and unstable dynamic system whose properties and related control strategies have been studied extensively in the control literature. A basic setup consists of a translation device – the cart – and a rotating boom – the pendulum – which is balanced in its upright position. The control algorithm uses the position of the cart and the rotation angle of the pendulum as input measurements provided by different sensors. While contacting sensor principles such as angle encoders have been used in different demonstrators, we present a purely vision-based tracking system. In combination with state of the art control algorithms our system is able to swing-up and balance the pendulum. The presented setup is non-contacting and does not require specific visual markers on any part of the pendulum. We use off-the-shelf components to realise the monocular tracking system. Experimental results show that our system is able to robustly control the inverted pendulum in real-time on a standard desktop PC.*

Keywords – *Tracking, Optical Metrology, Visual Feedback, Particle Filter*

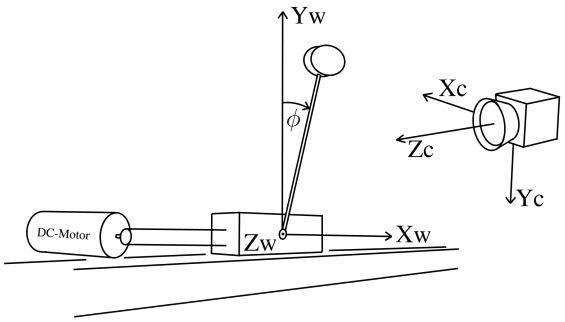

Fig. 1. Sketch of inverted pendulum. The aim of the experiment is to balance the pendulum in its upright position ($\phi = 0\,^\circ$) by means of providing control signals to the DC motor which in turn drives the supporting cart.

I. INTRODUCTION

The basic geometry of the inverted pendulum is shown in Figure 1. A control algorithm is used to drive the cart in order to balance the pendulum in its upright position. Due to its dynamic properties the inverted pendulum has become one of the classical examples in the literature used to develop and validate control algorithms for non-linear and unstable dynamic systems [1].

From a control perspective the position of the cart and the deviation of the pendulum from its upright position are relevant measurands in order to control the pendulum and to ensure that the cart remains within its allowed range of positions. Traditional sensors such as rotation angle encoders are frequently applied in this context [2]. These sensors provide robust measurement data but require mechanical coupling to the pendulum and electrical connections to the controller. An appealing property of vision-based measurement systems is the lack of feedback to the measurand. Hence, the dynamics of the inverted pendulum are not influenced by additional mass (e.g. the mass of a sensor) and friction (e.g. sensor cabling). Only few works target the vision-based control of an inverted pendulum. Wenzel *et al.* [3] present a demonstrator using dedicated markers that are detected in a sequence of camera images using pattern matching algorithms. The proposed structure only covers the control of the balancing pendulum but does not include the automatic swinging-up of the pendulum. Vision feedback is also used by Magana and Holzapfel [4] in a fuzzy logic control scheme. The algorithm used to deduce the position of the pendulum given a sequence of images puts severe restrictions on the positioning of the camera with respect to the pendulum. Martinez and Becerra [5] use optical flow as primary source of information to train and consequently apply an adaptive controller for the inverted pendulum task. This work is based on simulations in a virtual reality environment.

This paper presents a vision-based feedback system which extends the state of the art by providing the following features: First, the system properly handles full perspective distortions of the camera images. Thus, the camera can be placed anywhere in front of the demonstrator – visibility of the pendulum provided. A simple on-site calibration step is required to estimate the necessary parameters of this transformation. Second, a cascaded set of particle filters is used to track the cart and the pendulum. This particular combination enables robust track-

ing without the need of any visual markers on the demonstrator. Third, the proposed combination of a vision-based tracking system and a control algorithm is able to handle both the swinging-up process and the balancing process of the pendulum. Switching between the different control strategies is performed automatically using the pendulum energy.
In the subsequent sections an overview of our setup is given and experimental results showing the feasibility of our approach are presented.

II. INVERTED PENDULUM

For our developments we have designed and built a setup as sketched in Figure 1. A cart carrying the bearing of the pendulum slides along a set of rails. In this standard configuration the pendulum is free to rotate around this bearing. We use a DC motor to drive the cart. By construction the movement of the cart is restricted to a 1D translation along the X_W axis and the movement of the pendulum is restricted to a rotation around the Z_W axis. We use a $150\,\text{mm}$ rod with a $24\,\text{mm}$ diameter brass disk as pendulum and allow for a maximum translation of the cart of $560\,\text{mm}$. In the next paragraphs we outline the different control strategies and the measurement setup used to track and control the pendulum.

A. Control System

The state vector of the inverted pendulum is given by

$$\mathbf{x} = (x, v_x, \phi, \omega)^T, \tag{1}$$

where x and v_x denote the position and velocity of the cart, and ϕ and ω denote the angular position and the angular velocity of the pendulum, respectively. At any time, the inverted pendulum is in one of its two possible operating conditions: *Balancing* refers to the condition where the pendulum is balanced in its upright position (i.e. $\phi = 0\,^\circ$ in Figure 1). A linear quadratic regulator (LQR) [6] is applied to obtain the control signal u for the DC motor based on the state vector using a control law of the form

$$u = -\mathbf{k}^T\mathbf{x}. \tag{2}$$

The implementation of the LQR is based on a local linearisation of the dynamic model of the pendulum around the point of instability $\phi = 0\,^\circ$.
The second operating condition, termed *swinging-up*, is characterised by control commands that try to transition the pendulum to the balancing condition. In our setup an energy-based control law is used to swing-up the pendulum (cf. Åström and Furuta [7]). The control command for the DC motor is given by

$$u \propto -sat\left(\frac{E_{Top}}{E_{Pot} + E_{Rot}}\cos\phi sign(\omega)\right), \tag{3}$$

where E_{Top}, E_{Pot}, and E_{Rot} denote the potential energy of the pendulum at its top position, the current potential energy of the pendulum, and the current rotational energy of the pendulum. The function $sat(\cdot)$ ensures bounded control voltages by applying a signal saturation. Our controller automatically switches from *swinging-up* to *balancing* once $(E_{Pot}+E_{Rot}) = E_{Top}$ and the deviation of the angular position is less than a threshold, i.e. $|\phi| \leq \phi_{Switch}$.

B. Measurement Setup

The controller uses observations of the cart position and the pendulum rotation angle as inputs. We currently use two sets of sensors in order to allow for performance comparisons (cf. Section IV). Ground-truth data is provided by two angular position sensors AS5040 based on the Hall effect. Two magnetic dipoles are attached to the shaft of the DC motor and the bearing of the pendulum, respectively. The digital impulses delivered by the sensors allow us to accurately estimate both x and ϕ of the setup. A vision-based tracking system using data provided by a standard CCD camera with $640 \times 480\,\text{pixel}^2$ represents the main measurement system used in our experiments. The camera provides measurement updates at a rate of $30\,\text{Hz}$. Figure 1 also shows the position of the camera with respect to the cart. In order to deliver parameter estimates in a metric frame we calibrate the lens distortion model of the camera using a standard technique [8]. The correspondence between the measurement plane Π_M represented by $Z_W = 0$ and the image plane of the camera is established by means of a perspective homography [9]. 4 point correspondences within Π_M and their respective image points are used to estimate the homography parameters which are then used during measurement. This calibration is done once per camera position and allows us to freely move the camera to any position in front of the pendulum provided the out-most positions of the cart and the pendulum are still visible in the camera image.

III. VISION-BASED TRACKING

Vision-based tracking is concerned with the sequential estimation of measurands based on sequences of 2D images. In the case of the inverted pendulum we measure the position of the cart and the orientation angle of the pendulum, both measurands being part of the state vector $\mathbf{x}$. While algorithms exists that are capable of reliably tracking isolated passive [10], [11] or active [12], [13] markers, our tracking system operates without the use of markers.
Inherent to the marker-less tracking approach is the presence of ambiguity and noise. In particular, background clutter caused by non-homogeneous background conditions and the high degree of similarity between the visual footprint of the pendulum and its background require a tracking strategy that can robustly tackle multi-modalities in the observations and state representation. The use of stochastic tracking approaches is particularly useful in situations where both background and foreground of the objects can be modelled. Particle filters (PFs) as a representative of the family of Bayes filters have already been used in vision-based tracking applications where significant clutter and outliers are present [14]. In the following paragraphs we briefly outline the concept of PFs prior to giving an overview of the cascaded PF tracker used to track the state vector of the

inverted pendulum. A more general introduction to the topic of PF can be found in Arulampalam *et al.* [15].

A. Particle Filtering

Bayesian filters are used to estimate the inner state of a dynamic system by means of repeated observations. In general, the dynamic model of the system is given by

$$\mathbf{x}_k = f(\mathbf{x}_{k-1}, \mathbf{v}_k), \tag{4}$$

where $f(\cdot)$ represents a vector-valued function describing the state transitions and $\mathbf{v}_k$ denotes a noise component. A probabilistic representation of the state vector is used. Thus, the state vector $\mathbf{x}_k$ at time step k is fully described by its probability density function (pdf) $p(\mathbf{x}_k)$. Measurements are related to the state vector by

$$\mathbf{z}_k = h(\mathbf{x}_k, \mathbf{w}_k), \tag{5}$$

where again $h(\cdot)$ is a vector-valued function and $\mathbf{w}_k$ represents the measurement noise. Using the symbol $\mathbf{Z}_k = \{\mathbf{z}_1, \mathbf{z}_2, \dots \mathbf{z}_k\}$ to denote the history of all measurements obtained up to time k we can now formulate the Bayesian filter problem as the estimation of $\mathbf{x}_k$ knowing $\mathbf{Z}_k$.

In an iterative formulation the Bayes filter alternately performs *prediction* and *measurement* steps. The prediction step executes the state transition from time step $k-1$ to time step k. In other words, using conditional densities, the transition from $p(\mathbf{x}_{k-1}|\mathbf{Z}_{k-1})$ to $p(\mathbf{x}_k|\mathbf{Z}_{k-1})$. For first order Markov processes the current state depends only on its immediate predecessor so that the state transition in Equation 4 is fully characterised by the conditional density $p(\mathbf{x}_k|\mathbf{x}_{k-1})$. Applying the Chapman-Kolmogorov equation we obtain the *prior state density* – or *a priori* density – by

$$p(\mathbf{x}_k|\mathbf{Z}_{k-1}) = \int_\Omega p(\mathbf{x}_k|\mathbf{x}_{k-1}) p(\mathbf{x}_{k-1}|\mathbf{Z}_{k-1}) d\mathbf{x}_{k-1}. \tag{6}$$

Prior density in this context refers to the fact that the state density is expressed *prior to the measurement step* which is described next. Measurements are incorporated into the current estimate using Bayes law. The *posterior state density* is given by

$$p(\mathbf{x}_k|\mathbf{Z}_k) = \frac{p(\mathbf{z}_k|\mathbf{x}_k) \cdot p(\mathbf{x}_k|\mathbf{Z}_{k-1})}{p(\mathbf{Z}_k)}, \tag{7}$$

where $p(\mathbf{z}_k|\mathbf{x}_k)$ denotes the probabilistic formulation of the measurement process (cf. Equation 5). For Gaussian densities both the prediction step in Equation 6 and the measurement update in Equation 7 can be solved analytically leading to the well known Kalman filter algorithm [16]. However, in situations where densities deviate from the Gaussian case (e.g. multimodal state densities), the prediction and measurement steps can only be solved numerically. Particle filters (PFs) approximate state pdfs by means of stochastic samples. Thus, the pdf $p(\mathbf{x}_k)$ is approximated by

$$p(\mathbf{x}_k) \approx \{\mathbf{s}_k^{(m)}, \pi_k^{(m)}\} \qquad m = 1, \dots, N, \tag{8}$$

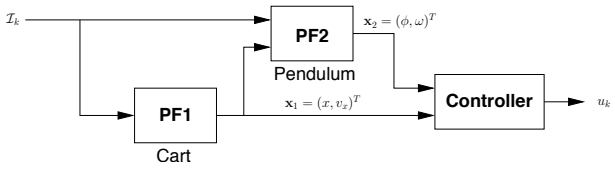

Fig. 2. Block diagram of the inverted pendulum control algorithm. Two Particle Filter trackers are uses to estimate the cart position and velocity (PF1) and the pendulum angle and angular velocity (PF2) given the most recent image $\mathcal{I}_k$. Based on these inputs the controller provides the control signal u_k for the DC motor.

where N denotes the number of samples. With increasing N the quality of this approximation improves and Equation 8 converges to the true pdf. Characteristic measures of the posterior pdf such as the first moment (i.e. a location parameter) can be straight forwardly obtained using

$$\hat{\mathbf{x}}_k = E\{\mathbf{x}_k|\mathbf{Z}_k\} \approx \sum_{m=1}^{N} \pi_k^{(m)} \mathbf{s}_k^{(m)}, \tag{9}$$

assuming normalised weights, i.e. $\sum_{m=1}^{N} \pi_k^{(m)} = 1$. Critical details of the PF filter are the resampling strategy and the incorporation of measurements. We will focus on these issues during the discussion of the cart and the pendulum tracker.

B. Cascaded Particle Filters

The number of samples used in Equation 8 has a direct impact on the robustness of the PF tracker. However, with increasing N the tracker will not only provide more stable results but also take a longer time during the measurement updates. In order to achieve real-time performance it is important to use as few samples as possible while still providing an approximation to the posterior density that is good enough for controlling the inverted pendulum. We use two individual tracking modules for the cart and the pendulum. This separation reduces the dimensionality of the state vector and allows us to apply resampling strategies tailored to the specific object. Figure 2 shows a diagram of the tracking and control structured realised in this work. Based on an acquired image covering both the cart and the pendulum the tracker PF1 provides an estimate for the cart position x and velocity v_x. We use the output PF1 to initialise search regions in PF2 devoted to the tracking of the angular position ϕ and velocity ω of the pendulum.

C. Tracking of the Cart

By construction of the cart it can only translate within Π_M along a trajectory parallel to the X_W axis. Using the homography estimated during the setup of the camera (cf. Section II) this trajectory can be projected into a linear trajectory in image space. We use $N = 100$ samples to approximate the posterior density $p(\mathbf{x}_1)$ (cf. Figure 2). In order to improve the convergence behaviour of the state estimate and to ensure timely

recovery of the cart after visual occlusions, 25 % of the samples are obtained in an importance sampling step [14]. Importance sampling tries to sample the state space where the position of the cart is most likely. As an importance measure the correlation of the image pixels along the cart trajectory with a template function $t(x)$ is used. We obtain the template by projecting an approximation of the cart's visual footprint onto the image plane.

Measurement updates focus on the visual contour of the cart. In order to update each individual sample weight we measure the edge position along $L = 16$ measurement lines as outlined in Figure 3a. Each of these measurement lines has a length of D pixels in the image domain. Assuming that the gradient-based edge detection of measurement line l results in R_l contour candidates z_r, we obtain a new sample weight

$$\pi_k = \prod_{l=1}^{L} \frac{\sum_{r=1}^{R_l} \frac{1}{\sqrt{2\pi}\sigma} e^{-\frac{(z_r - D/2)^2}{2\sigma^2}}}{e^{-\lambda D} \frac{(\lambda D)^{R_l}}{R_l!}}. \qquad (10)$$

This equation includes a Gaussian measurement model and a Poisson background model. The individual parameters σ and λ depend on the measurement setup and have been identified experimentally. A kernel density estimator [17] is applied to determine the best estimate of the unknown elements of the state vector.

D. *Tracking of the Pendulum*

Similar to the cart, the pendulum is tracked using a separate PF. During the measurement $L = 8$ measurement lines as shown in Figure 3b are used. Again a 1D edge detection algorithm is applied along each measurement line and the combination of the obtained foreground/background ratios are used to obtain an update for the weight of the sample as shown in Equation 10. We apply an importance sampling strategy using a correlation measure evaluated along the possible orientations of the pendulum. Knowing the centre of the bearing as a result of PF1 and the geometry of the pendulum the set of possible positions of the pendulum describes an ellipse in the image plane. For the pendulum, too, we use $N = 100$ samples with a a portion of 25 % as importance samples.

IV. EXPERIMENTS

The presented vision-based tracking system has been implemented on a standard desktop PC (Intel Core2 1.86 GHz) running the Linux operating system. Hall sensors used to determine the position and the orientation of the pendulum have been added for reference purposes. A CPLD logic interfaces the sensor data to the PC via a general purpose digital I/O interface. Figure 4 shows a close-up of the demonstrator.

In our experiments the vision-based tracker has provided state estimates at frame-rate (i.e. 30 fps). This update rate is sufficient to balance the pendulum in its upright position in our setup. The elements of the state vector estimated during a period of 15 s are shown in Figure 5. In this particular experiment two aspects of our implementation have been validated: First, the proper switching between the initialisation and the balancing control law is discussed. After launching the application the controller tries to bring the pendulum in the upright position. At time $t \approx 7.5$ s the application automatically switches from the P-control law to the LQR control law. The pendulum is successfully balanced in the upright position until the end of the experiment. The second aspect of this experiment is the comparison between the Hall sensor readings and the vision-based measurements obtained by PF1 and PF2. The deviations between these signals are shown for x and ϕ in Figure 5b and d, respectively.

The outliers represented by spikes in the deviation measures are caused by two effects: First, the acquired measurement signals from the Hall sensors and the vision-based tracker do not correspond to exactly the same time instances due to the latency introduced by the image acquisition system (camera, firewire bus). Second, we observe a model mismatch between the true object dynamic and the motion model used by the PF. This can not be avoided - in particular during the change between swing motion and constant position of the pendulum. However, the experiments show that the quality of the estimated state vector is sufficient to balance the pendulum.

We have performed experiments to determine the optimal size of the importance sample set. For $N = 100$ samples used by both the cart and the pendulum particle filter, $N_{\mathrm{IS}} = 25$ importance samples showed to be a good trade-off between computational complexity and robustness of the resultant tracking algorithms. Figure 6 shows the different types of samples (standard resampling, importance sampling, initialisation) and the corresponding contour detections superimposed to a single frame captured by the camera. It is evident that although false positives appear (e.g. at the window in the background on the left of the image), the true cart and pendulum positions are successfully tracked.

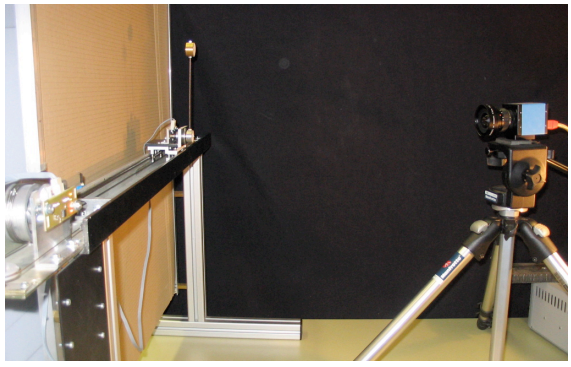

Fig. 4. Inverted pendulum prototype. The cart, pendulum, and parts of the driving DC motor are shown on the left. A firewire camera is used to provide visual feedback for the control algorithm. In this prototype both vision-based tracking and commercially available Hall sensors can be used to measure the state of the pendulum.

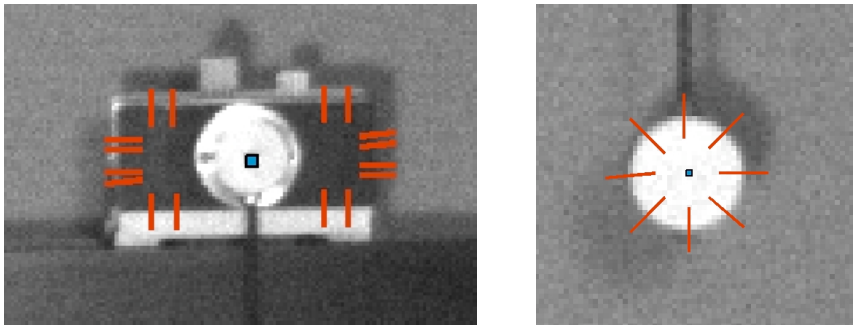

(a) (b)

Fig. 3. Measurement models. (a) 16 measurement lines are used to identify and track the cart. (b) 8 radially symmetric measurement lines are used for the pendulum. In both cases the sample that gave rise to the measurement lines is depicted as blue square.

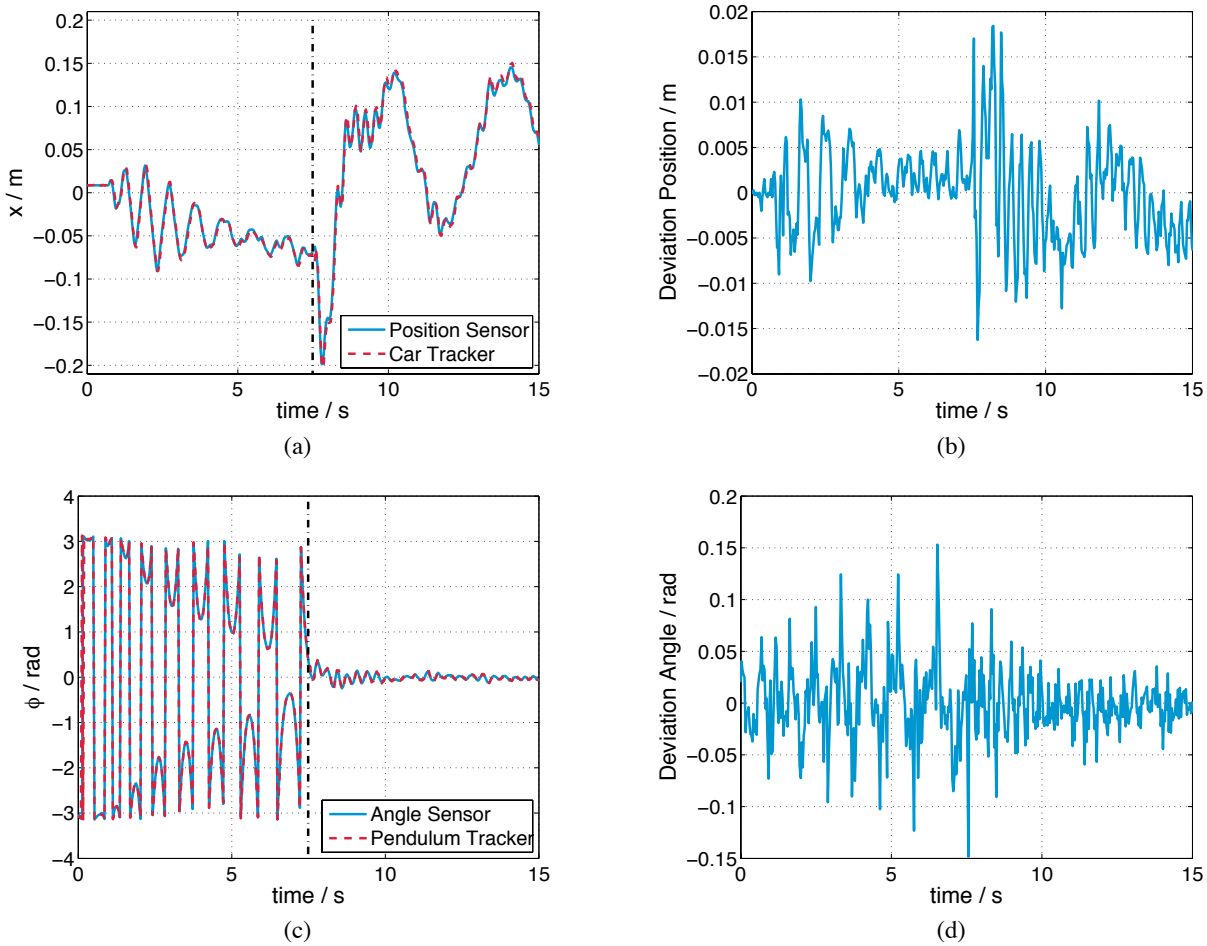

Fig. 5. Measurement results of the vision-based tracking algorithm. (a) Position of the cart measured by the Hall sensor and the particle filter PF1. The deviations of the PF1 result w.r.t. the Hall sensor are shown in (b). (c) Orientation angle of the pendulum as observed by the Hall sensor and PF2. Again, deviations are shown in (d). The vertical lines at $t \approx 7.5\,\mathrm{s}$ in (a) and (c) denote the point where the application switches between swinging-up and balancing of the pendulum.

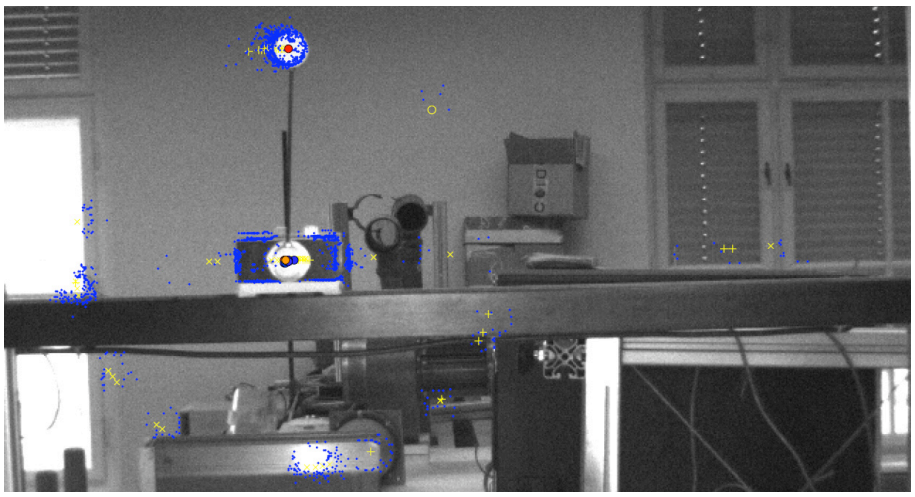

Fig. 6. Different types of samples (yellow) and the resultant contour detections (blue) superimposed to a camera frame: Standard resampling (+), importance sampling (x), and initialisations (o). Samples used by the cart tracker are distributed horizontally along the cart track while samples used by the pendulum are distributed along the ellipse centred at the cart representing possible pendulum locations.

V. CONCLUSION

In the present paper we report on the design and implementation of a vision-based system used to control an inverted pendulum. While we employ standard algorithms to obtain a control output for the different operating conditions of the pendulum, the novelty of our approach lies in the specific use of a set of cascaded particle filter trackers. Our approach is characterised by the absence of any artificial landmarks. Further, only a simple calibration step is required in order to obtain stable tracking results using a monocular camera setup at an arbitrary position in front of the pendulum. Through the use of a contour-based measurement process, our system only requires a minimum visual contrast between the pendulum or cart and the background. The system performs both initialisation and balancing of the pendulum using automated switching between different control laws. Experimental results using an implementation on a standard PC show that the vision-based tracking algorithm provides unbiased estimates of the pendulum's state vector and is sufficiently robust to control the pendulum.

ACKNOWLEDGEMENTS

This work was supported by the Austrian Science Foundation (FWF) under grant No. S9103-N13.

BIBLIOGRAPHY

[1] G. F. Franklin, J. D. Powell, and A. Emami-Naeini, *Feedback Control of Dynamic Systems*, Number ISBN 0130323934. Prentice Hall, 2002.

[2] Z. Lin, A. Saberi, M. Gutmann, and Y. A. Shamash, "Linear controller for an inverted pendulum having restricted travel: a high-and-low gain approach," *Automatica*, vol. 32, no. 6, pp. 933–937, 1996.

[3] L.Wenzel, N. Vazquez, D. Nair, and R. Jamal, "Computer vision based inverted pendulum," in *Instrumentation and Measurement Technoloqy Conference*, 2000, vol. 3, pp. 1319–1323.

[4] M.E. Magana and F. Holzapfel, "Fuzzy-logic control of an inverted pendulum with vision feedback," in *IEEE Transactions on Education*, May 1998, vol. 41, pp. 165–170.

[5] G. Martinez-Hernandez and V.M. Becerra, "Preliminary results from a real time control system using optical information," in *Systems, Man and Cybernetics*, October 2004, vol. 6, pp. 5923–5928.

[6] C.-T. Chen, *Analog and digital control system design: Transfer-Function, State-Space, and Algebraic Methods*, Number ISBN 0-03-094070-2. Saunders College Publishing, 1993.

[7] K.J. Åström and K. Furuta, "Swinging up a pendulum by energy control," in *Automatica*, February 2000, vol. 36, pp. 287–295.

[8] "Caltech Camera Calibration Toolbox for MATLAB," http://www.vision.caltech.edu (10.11.2007).

[9] R. I. Hartley and A. Zisserman, *Multiple View Geometry in Computer Vision*, Cambridge University Press, 2^{nd} edition, 2004.

[10] H. Kato, M. Billinghurst, I. Poupyrev, K. Imamaoto, and K. Tachibana, "Virtual object manipulation on a table-top ar environment," in *Proc. of the International Symposium on Augmented Reality (ISAR 2000)*, Munich, Germany, 2000, pp. 111–119.

[11] L. Naimark and E. Foxlin, "Circular data matrix fiducial system and robust image processing for a wearable vision-inertial self-tracker," Darmstadt, Germany, 2001.

[12] M. Ribo, A. Pinz, and A. L. Fuhrmann, "A new Optical Tracking System for Virtual and Augmented Reality Applications," in *Proc. of IEEE Instrumentation and Measurement Technology Conference, IMTC 2001*, Budapest, Hungary, May 2001, vol. 3, pp. 1932–1936.

[13] K. Dorfmüller, "Robust tracking for augmented reality using retroreflective markers," vol. 23, no. 6, pp. 795–800, December 1999.

[14] M. Isard and A. Blake, "ICondensation: Unifying low-level and high-level tracking in a stochastic framework," in *Proc. of European Conference on Computer Vision (ECCV)*, 1998.

[15] M. S. Arulampalam, S. Maskell, N. J. Gordon, and T. Clapp, "A tutorial on particle filters for online nonlinear/non-gaussian bayesian tracking," *IEEE Trans. on Signal Processing*, vol. 50, no. 2, pp. 174–188, 2002.

[16] R.E. Kalman, "A new approach to linear filtering and prediction problems," *Transactions of the ASME–Journal of Basic Engineering*, pp. 35–45, March 1960.

[17] C. Chang and R. Ansari, "Kernel particle filter: iterative sampling for efficient visual tracking," in *IEEE International Conference on Image Processing (ICIP'03)*, September 2003, vol. 3, pp. 977–980.